

# Bond durability of concrete-CFRP EBR and NSM systems under natural ageing

Ricardo Cruz<sup>1</sup>, Luís Correia<sup>2</sup>, Susana Cabral-Fonseca<sup>3</sup>, José Sena-Cruz<sup>4,\*</sup>

1. PhD Student, Dep. of Civil Engineering of University of Minho, ISISE/IB-S, Guimarães, Portugal

2. Post-doctoral researcher, Dep. of Civil Engineering of University of Minho, ISISE/IB-S, Guimarães, Portugal

3. Research Officer, Materials Department, Laboratório Nacional de Engenharia Civil, Lisboa, Portugal

4. Associate Professor, Dep. of Civil Engineering, University of Minho, ISISE/IB-S, Guimarães, Portugal

\*Corresponding author email: jsena@civil.uminho.pt

## Abstract

The use of Carbon Fibre Reinforced Polymer (CFRP) as reinforcement material for strengthening of existing reinforced concrete (RC) structures has been increasing. These materials can be applied mainly by using two strengthening techniques: (i) the Externally Bonded Reinforcement (EBR) by the application of the CFRP on the concrete surface; and, (ii) the Near Surface Mounted (NSM) by the insertion of the CFRP into the grooves on the concrete cover of the RC element to be strengthened.

The durability of structures strengthened with CFRP materials is still an open issue. Accelerated ageing protocols under laboratory conditions have been used for the assessment of the durability; however, very few studies have been performed in outdoor environments (natural ageing). Moreover, the relationship between accelerated ageing and real outdoor ageing is not fully understood.

The main objective of this paper is to give new insights on the bond durability between concrete and CFRP strips installed according to both EBR and NSM techniques, after a 2-year exposure to natural outdoor conditions. This study includes a reference environment ( $\sim 20\text{ }^{\circ}\text{C}$  / 55% RH) for comparing proposes and four outdoor environments for ageing induced mainly promoting (i) carbonation, (ii) freeze-thaw attack, (iii) elevated temperatures, and (iv) airborne chlorides from seawater. An additional environmental condition, namely continuous immersion in water at  $\sim 20\text{ }^{\circ}\text{C}$  was also considered.

The performance of the bond concrete-adhesive-CFRP was assessed throughout pull-out tests. When compared with the reference environment, small degradation on the bond performance on specimens exposed to outdoor environments has been observed for both strengthening techniques.

**Keywords:** *bond, EBR, NSM, durability, natural outdoor ageing.*

# 1. Introduction

In the last decades, the application of fibre reinforced polymer (FRP) materials for strengthening of existing reinforced concrete (RC) structures has been growing. These composite materials can be applied according to externally bonded reinforcement technique (EBR) or near-surface-mounted technique (NSM). The durability of RC structures strengthened with CFRP materials has been intensively studied under laboratorial conditions (accelerated ageing tests). Nevertheless, several gaps in the existing knowledge can be found, mainly about the performance of this type of strengthening solutions under outdoor conditions (natural ageing). Another important topic that needs to be better understood is the relationship between the effects of accelerated ageing and natural ageing, (Tatar and Hamilton 2016). A few publications can be found addressing this topic in literature. In these publications, some include both types of exposure and also attempts to establish relationships between both types of exposure are provided, e.g. (Tatar and Hamilton 2016; Kabir et al. 2016; Hassan et al. 2015; Mohd Hashim et al. 2016; Fernandes et al. 2018). Other publications only address the durability under outdoor conditions (Hsieh et al. 2016; Sen 2015; Al-Tamimi Adil et al. 2015; Bhashya et al. 2015). In general, the level of degradation observed with accelerated ageing in laboratorial conditions is higher than in natural ageing for similar ageing durations.

This paper presents the results of an investigation on the durability of bond between CFRP laminates and concrete subjected to four outdoor environments inducing ageing mainly by carbonation, freeze-thaw attack, elevated temperatures, and airborne chlorides from seawater for a period of two years of exposure. It should be noted the presence of ultraviolet radiation from the sun in these outdoor environments. A control (reference) environment and an environment involving water immersion of the materials under controlled temperature (20 °C) were also included. The bond behaviour was characterized after specimen's production and after the mentioned exposure.

## 2. Experimental program

### 2.1. Overview

The experimental program was carried out in the framework of the project “FRPLongDur - Long-term structural and durability performances of reinforced concrete elements strengthened in flexure with CFRP laminates”, which intends to investigate the long-term structural behaviour and durability of reinforced concrete (RC) elements strengthened in flexure with CFRP laminates under relevant artificial and outdoor environments. This project includes several types of specimens for durability assessment at a different scale levels: (i) samples of the materials (concrete, epoxy adhesives and CFRP laminates), (ii) bond specimens (EBR and NSM techniques) and (iii) full-scale RC slabs strengthened in flexure with CFRP laminates (EBR and NSM techniques). The present paper addresses the results of the durability of the bond specimens.

Six different environments are considered, namely: two artificial environments (E1 and E2) and four outdoor environments (E3 to E6). The E1, with controlled hygrothermal conditions (20 °C/55% RH), was considered as the reference environment; E2 intends to understand the effect immersion in water with controlled temperature (~20 °C). Both artificial environments were installed at the University of Minho, Guimarães. The outdoor environments are located in Portugal, being expected to achieve specific ageing conditions in each one, namely: E3 – higher levels of concrete carbonation, due to the levels of CO<sub>2</sub> concentration, as these specimens were placed in the National Laboratory of Civil Engineering (LNEC), Lisbon (38°45'41.7"N 9°08'30.6"W), near the International Airport of Lisbon and near a highway with heavy traffic load; E4 – freeze-thaw cycles, since these specimens were placed near the highest mountain of Portugal (‘Serra da Estrela’), at Lagoa Comprida’s Dam, Seia (40°21'55.8"N 7°38'52.0"W); E5 – higher (elevated) service temperatures and lower relative humidity as these specimens were placed at premises of the Factory of S&P Clever and Reinforcement, located in Elvas (38°53'33.5"N 7°08'46.0"W); E6 – higher levels of chlorides concentration and relative humidity, since these specimens were placed in the Port of Viana do Castelo (APDL), Viana do Castelo (41°40'57.0"N 8°49'28.3"W), near the Atlantic Ocean. Figure 1 present the specimens installed in two of the six environments.



Figure 1. Aspects of the specimens in the stations (a) E3 and (b) E4.

The production of the specimens required several steps, being completed approximately 14 months (March 2017) before the beginning of installation in the corresponding environments (May 2018). During this period, all the specimens were kept in the laboratory environment. An initial assessment of the bond mechanical properties (4 tests per strengthening technique) was performed 8 months after specimen's production (October 2017). The installation of the specimens in each environment took place between June 2018 and December 2018.

After two years of exposure, 24 specimens (4 from each environment) were collected and tested. The test protocol included a desorption period during 3 weeks with the hygrothermal conditions defined for E1. In the case of E2 specimens (immersed in water), no desorption phase was considered and all specimens were kept fully immersed being removed immediately before testing.

To record the ambient temperature and relative humidity, sensors were installed in each experimental station (typical characteristics of the sensors: temperature range/resolution of  $-35$  to  $+80$  °C/ $0.5$  °C; humidity range/resolution of  $0$  to  $100\%$ / $0.5\%$ ). Some sensors faced technical issues, being the missing information provided by Portuguese Institute for the Sea and Environment (IPMA). Table 1 presents the average ambient temperatures and relative humidity recorded between the years of 2018 and 2020 for each environment and trimester.

Table 1. Values of the average temperature and relative humidity registered between the years 2018 and 2020 for the different environments studied.

Environment		Year 2018		Year 2019				Year 2020			
		Jul-Sep	Oct-Dec	Jan-Mar	Apr-Jun	Jul-Sep	Oct-Dec	Jan-Mar	Apr-Jun	Jul-Sep	Oct-Dec
E1	Temp. [°C]	20.5	18.6	20.5	20.1	20.0	20.1	20.2	20.2	--	--
	RH [%]	69.9	62.7	50.7	60.6	71.5	63.8	54.3	62.5	--	--
E2	Temp. [°C]	24.3	21.4	20.6	21.2	21.6	19.8	20.0 <sup>(3)</sup>	20.0 <sup>(3)</sup>	--	--
	RH [%]	100.0	100.0	100.0	100.0	100.0	100.0	100.0	100.0	--	--
E3	Temp. [°C]	22.2 <sup>(1)</sup>	15.3	17.1	17.9	22.0	15.7	13.6	14.9	--	--
	RH [%]	66.2 <sup>(1)</sup>	78.5	71.0	67.1	66.8	81.6	78.3	80.5	--	--
E4 <sup>(2)</sup>	Temp. [°C]	18.0	7.8	5.8	10.2	17.1	7.7	6.1	11.5	--	--
	RH [%]	60.3	78.8	63.9	71.4	59.4	80.5	75.3	79.6	--	--
E5 <sup>(2)</sup>	Temp. [°C]	26.1	13.2	10.9	19.3	25.0	14.5	11.6	19.2	--	--
	RH [%]	49.1	79.8	69.7	54.6	48.5	75.8	78.2	66.5	--	--
E6	Temp. [°C]	--	--	12.1	17.9	21.8	13.7	12.6	19.0	22.5	14.2
	RH [%]	--	--	76.1	69.0	71.0	88.1	82.8	75.8	70.2	86.7

Notes: <sup>(1)</sup> Also considered 26-30 June 2018; <sup>(2)</sup> Values obtained from IPMA (the IPMA's location station is 9 km apart E3 and 560 m apart E5); <sup>(3)</sup> Values obtained from controller equipment installed in the 7<sup>th</sup> trimester on the experimental station.

## 2.2. Material characterization

The assessment of the mechanical properties of the used materials was performed. The results obtained for concrete, adhesive and CFRP laminates are presented in Table 2. Regarding the concrete, all specimens were cast using a single batch. In order to evaluate the compressive strength and elastic modulus at the age of 28 days, four cylindrical concrete specimens with 150/300 mm (diameter/height) were used, through the NP EN 12390-3:2011 and NP EN 12390-13:2014 standards, respectively. The mechanical properties of the adhesive (*S&P Resin 220 epoxy adhesive* supplied by *S&P® Clever Reinforcement Ibérica Lda Company*) were assessed after 7 days of curing, testing six “dog-boned shaped” specimens according to EN ISO 527-2:2012 recommendation. Finally, the mechanical properties of the CFRP laminate (produced by *S&P® Clever Reinforcement Ibérica Lda Company* with the trademarked CFK 150/2000) were also evaluated for the two cross-section geometries used. For each one, six samples were used according the EN ISO 527-5:2009 recommendation.

Table 2. Average results of material characterization.

Material	Mechanical properties			
Concrete	$f_{cm}$ [MPa] (CoV [%])	$E_{cm}$ [GPa] (CoV [%])	--	
	41.5 (4.4)	29.1 (4.7)	--	
Adhesive	$f_a$ [MPa] (CoV [%])	$E_a$ [GPa] (CoV [%])	$\varepsilon_a$ [ $\times 10^{-3}$ ] (CoV [%])	
	19.9 (3.0)	6.5 (3.0)	$4.0 \times 10^{-3}$ (6.2)	
Laminates	$f_f$ [MPa] (CoV [%])	$E_f$ [GPa] (CoV [%])	$\varepsilon_f$ [ $\times 10^{-3}$ ] (CoV [%])	
	CFRP_L10	2405 (3.8)	164 (1.2)	$14.6 \times 10^{-3}$ (3.8)
	CFRP_L50	2527 (10.8)	190 (9.3)	$13.3 \times 10^{-3}$ (13.6)

## 2.3. Specimens and test configuration

### 2.3.1. EBR

Figure 2 presents the geometry of EBR bond specimens and the corresponding test configuration. A concrete prism with  $400 \times 200 \times 200$  [mm] was used, being applied two CFRP laminate strips with a cross-section of  $50 \times 1.2$  mm<sup>2</sup> (L50) in opposite faces (parallel to the casting direction) according to the EBR technique. A bond length of 220 mm was adopted, with 100 mm free from the extremity of the concrete prism to avoid premature failure by concrete rip off ahead of the loaded end. The used bond length (220 mm) is higher than the theoretical effective length,  $l_e$ , of 101 mm (CNR 2013). In order to perform the pull-out tests, the specimens were placed horizontally on a steel plate with  $70 \times 300 \times 550$  [mm] identified as Support 1, which was fixed to the stiff base of the testing steel frame system through eight M16 steel threaded rods. A steel plate identified as Support 2 was placed in the bottom front part of the concrete block to assure negligible horizontal displacements of the specimen in the loading direction during the test, which acted as a reaction element at a height of 50 mm. The Support 3, which is a prismatic steel plate, was placed in the rear top part of the specimen to minimize vertical displacements during the test. Support 2 and Support 3 were fixed to the Support 1 through two M20 steel threaded rods. The tests were performed using a servo-controlled equipment and the applied force was measured through a load cell of 200 kN maximum load carrying capacity (linearity error of 0.05% F.S.), placed between the actuator and the grip used to pull the CFRP laminate during the test. The relative displacement between the CFRP and the concrete (slip) at the loaded end section ( $s_l$ ) and free end section ( $s_f$ ) was measured using the linear variable displacement transducers (LVDT) LVDT1 and LVDT2, respectively, with a stroke of  $\pm 10$  mm (linearity error of 0.24% F.S.). The tests were performed under displacement control at the loaded end through LVDT1 with a rate of 2  $\mu$ m/s. Additionally, a series of four strain gauges TML BFLA-5-3-3L were placed along the CFRP laminate centreline to measure the longitudinal strains during the loading process.

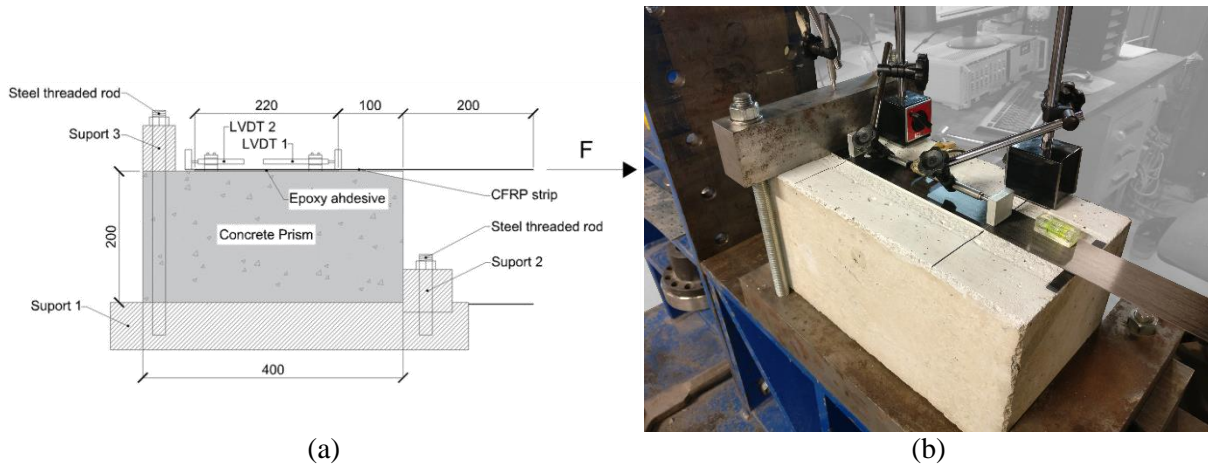


Figure 2. (a) Specimen's geometry and test configuration, and (b) photograph of the EBR bond test. Note: All units in [mm].

### 2.3.2. NSM

The performance of bond in NSM specimens was assessed performing direct pull-out tests. Figure 3 presents the geometry of NSM bond specimens and the respective test configuration. A concrete cubic block with 200 mm of edge was adopted, being applied a CFRP laminate strip of  $10 \times 1.4$  [mm] (L10) along a bond length of 60 mm. The CFRP strip was inserted in the centre of a groove with  $15 \times 5$  [mm] opened at the surface of the concrete block. The bond length was adopted to (i) avoid the failure of CFRP and (ii) be sufficiently large to be representative of the system and minimize the influence of the inevitable effects, as demonstrated in previous research (Fernandes et al. 2018). To apply the load, a servo-controlled equipment was used. To measure the slip at the loaded and free end, two LVDTs (range  $\pm 2.5$  mm and linearity error of  $\pm 0.05\%$  F.S.) were used, respectively LVDT1 and LVDT2. The load,  $F$ , was measured by a load cell placed between the grip and the actuator, with a static load carrying capacity of 200 kN (linearity error of  $\pm 0.05\%$  F.S.). The tests were performed under displacement control at the loaded end section (LVDT1), at a rate of  $2 \mu\text{m/s}$ .

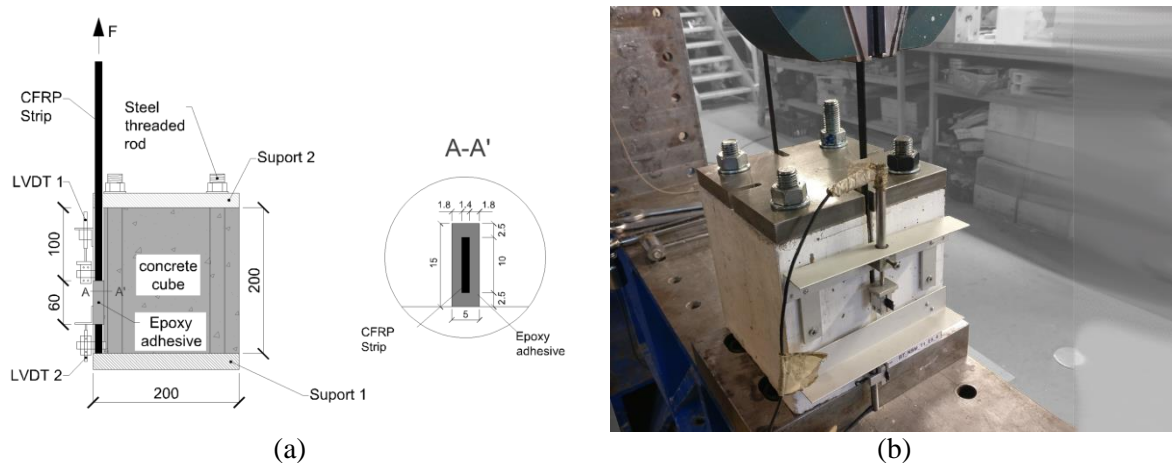


Figure 3. (a) Specimen's geometry and test configuration, and (b) photograph of the NSM bond test. Note: all units in [mm].

## 3. Results and discussion

This experimental campaign includes 28 specimens for each studied strengthening technic (4 specimens for the initial characterization and 24 specimens for characterization after two years of exposure, 4 for each environment) for assessing the durability of bond performance of EBR and NSM techniques.

### 3.1. Initial characterization

Table 3 present the main results obtained in the initial characterization on EBR and NSM bond specimens, namely the maximum force achieved during the test,  $F_{\max}$ , and corresponding slip in the loaded end,  $s_{\max}$ , and the failure mode observed.

Table 3. Main results of EBR and NSM bond tests of the initial characterization (average results of 4 specimens).

Strengthening technique	$F_{\max}$ [kN] (CoV [%])	$s_{\max}$ [mm] (CoV [%])	Failure Mode
EBR	30.2 (13.3)	--	F/A + C (2); C (2)
NSM	28.2 (2.5)	0.5 (5.7)	F/A (4)

Failure Modes: F/A = Debonding at laminate-adhesive interface; C = Cohesive failure of concrete; the values between brackets are the number of specimens where this failure mode occurred.

The pull-out test on EBR specimens presented an average maximum shear force of 30.2 kN, with the dominant failure mode of cohesive failure of the concrete (C). Additionally, in 2 specimens, in approximately half of the bond length, debonding at laminate adhesive-interface (F/A) was also observed. The average maximum strength obtained was equal to 503 MPa (~20% of the CFRP laminate tensile strength), which is in accordance with the formulation proposed in CNR (CNR 2013), where the expected maximum strength immediately before the CFRP debonding is equal to 505 MPa. Thus, a good correlation between the experimental and the expected maximum strength was observed. Failure modes are detailed in Section 3.2.

The average maximum pull-out force reached in NSM specimens was 28.2 kN. This value corresponds to a stress level of 2014 MPa, which represents around 70% of the CFRP laminate tensile strength. All tested specimens experience the same failure mode, i.e. debonding at the laminate-adhesive interface (F/A). Comparing both strengthening techniques, it is clear that the NSM system can achieve higher ultimate stress levels than the EBR system, with a smaller bond length. Failure modes are detailed in Section 3.2.

### 3.2. Characterization after two years of exposure

#### 3.2.1. EBR

Table 4 presents the average results of pull-out tests on EBR specimens (each environment and each time of testing includes 4 single specimens) after two years of environmental exposition. In this table,  $F_{\max}$  is the maximum shear force attained during the test. Failure modes observed are also presented, being detailed in Figure 5. Figure 4a presents the representative shear force *versus* loaded end slip relationships ( $F_1 - s_1$ ) for each environment (from the 4 tests, one curve was chosen to be presented) in the experimental campaign after two years of exposure. These curves presented the expected behaviour in pull-out on EBR specimens: first there is an ascending branch, with decreasing stiffness, then, the debonding load is reached (maximum load supported by the effective length according to (CNR 2013)), and the loaded end slip increases until failure (Soares et al. 2019; Mazzotti et al. 2016; Iovinella et al. 2013). Figure 4b shows a graphical representation of the maximum shear force obtained from the pull-out tests on EBR specimens on the initial characterization and after two years of exposure in the different environments.

The results obtained on the initial characterization are in agreement with the results of similar works, e.g. (Soares et al. 2019). The greatest decrease in  $F_{\max}$  (-8.3%, when compared with the initial characterization) was observed under the controlled environment E1, after two years of exposure. Considering that the dominant failure mode was cohesive on the concrete (see Figure 5), this observation is most likely due to variations on the mechanical properties of the concrete substrate. Comparing the values of  $F_{\max}$  obtained on E2-E6 specimens after two years of exposure with the initial characterization, the highest increase in  $F_{\max}$  (+16.2%) was verified in E3 environment, while in E4 the increase was +13.6%. Also, an increase was obtained in E2 (3.0%), and smaller decreases were verified in E5 (-0.3%) and E6 (-3.3%). Water can cause plasticization and swelling in epoxy adhesives, leading to considerable reductions on the elastic modulus and resistance, as described in the literature, e.g. (Cabral-Fonseca et

al. 2018; Sousa et al. 2018). Yet, it should be highlighted that, the immersion in water (E2 environment) and testing in a saturated state do not seem to affect the bond performance in EBR specimens. This finding can be related with the adhesive plasticization, which may reduce the interfacial stress peaks and lead to a more uniform distribution of stresses along the bond length, increasing the maximum force. Regarding to the increase of maximum force in outdoor environments, the reason for such observation can be related with the adhesive post-curing that may occur during the exposure period. Figure 5 presents the failure modes observed in bond EBR tests. The dominant failure mode after two years of exposure was cohesive failure in the concrete. In fact, only in one specimen, cohesive failure in the concrete with simultaneous debonding at the laminate-adhesive interface was also observed, as it is shown in Table 4. No significant differences between failure modes were observed with the type of exposure.

Table 4. Main results of pull-out tests on EBR specimens after two years of exposure to the environment studied (E1 to E6) (average results of 4 specimens).

Environment	$F_{max}$ [kN] (CoV [%])	Failure Mode
E1	27.7 (11.0)	C (4)
E2	31.1 (10.0)	C (3); C + F/A (1)
E3	35.1 (9.1)	C (4)
E4	34.4 (11.1)	C (4)
E5	30.1 (5.9)	C (4)
E6	29.2 (6.0)	C (4)

Failure modes: C = cohesive failure of concrete; C + F/A = cohesive failure of concrete and debonding at laminate-adhesive interface; values between brackets are the number of specimens where this failure mode occurred.

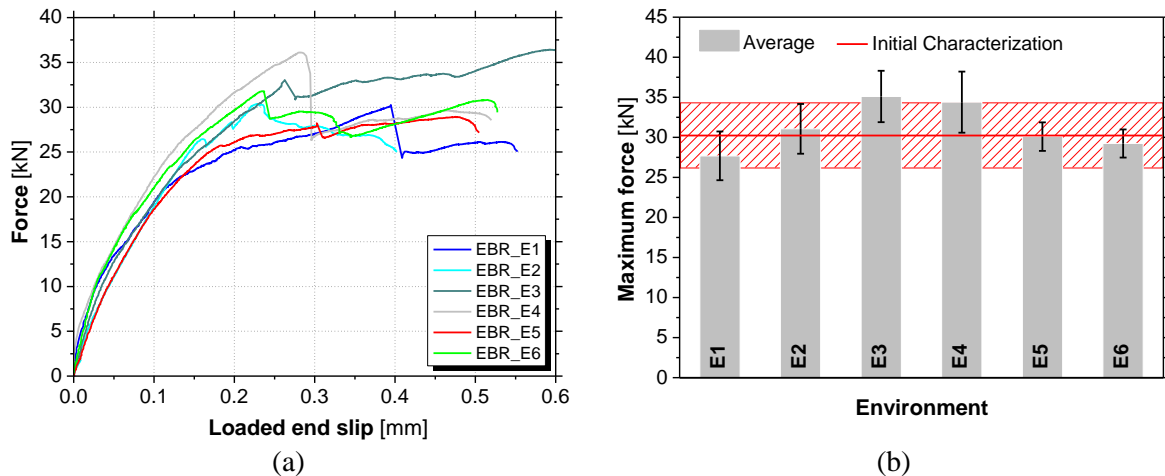


Figure 4. (a) Shear force vs. loaded end slip relationships obtained in bond EBR tests in each environment (representative curves) and (b) maximum shear force obtained on bond EBR tests after two years of exposure in each environment, including the initial characterization.

### 3.2.2. NSM

Table 5 presents the average results of pull-out tests (each environment and each time of testing includes 2 specimens; 4 tests) on NSM specimens after two years of environmental exposition. In this table,  $F_{max}$  is the maximum pull-out force attained during the test and  $s_{lmax}$  is the loaded end slip at  $F_{max}$ . Failure modes observed are also presented. Figure 6a presents the average pull-out force versus loaded end slip relationships ( $F_l - s_l$ ) for all the environments (average curve of 4 tests) obtained after two years of exposure. The typical shape observed in these curves was already observed in similar works (Fernandes et al. 2018; Fernandes et al. 2015; Ricardo Cruz et al. 2020). Mainly two branches can be observed, an ascending pre-peak branch and a descending post-peak branch. Although there are great similarities between these curves, results show some variations of  $F_{max}$  and respective  $s_{fmax}$  in each environment. Figure 6b presents a graphical representation of the maximum pull-out force for NSM specimens exposed to the different environments in the initial characterization and after two years of exposure.



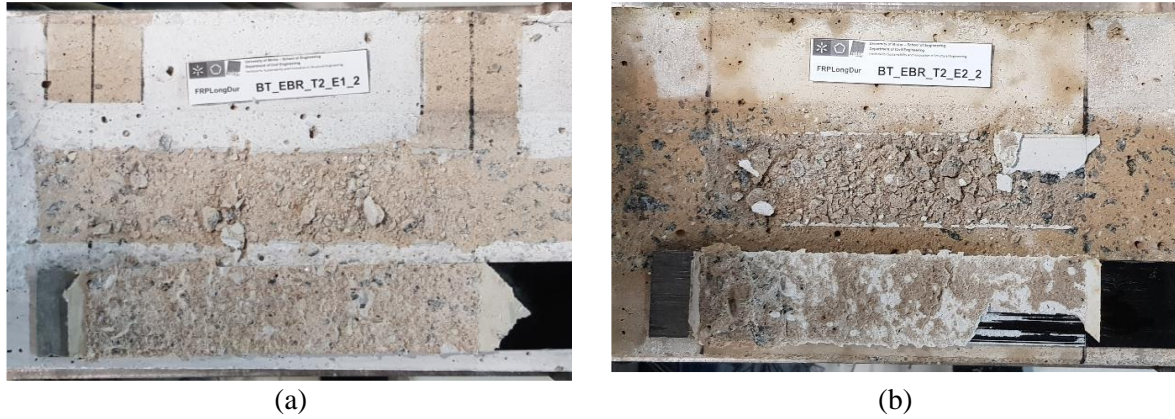


Figure 5. Typical observed failure modes in bond EBR tests: (a) cohesive failure of concrete – C and (b) cohesive failure of concrete and debonding at laminate-adhesive interface - C + F/A.

Table 5. Main results of pull-out tests on NSM specimens after two years of exposure to the studied environments (E1 to E6) (average results of 4 specimens).

Environment	$F_{max}$ [kN] (CoV [%])	$S_{max}$ [mm] (CoV [%])	Failure Mode
E1	28.0 (1.6)	0.6 (10.3)	F/A + CC (1); F/A (3)
E2	24.6 (2.0)	0.5 (21.0)	F/A + CS (2); F/A+ F/C + CS (1); A + CS (1)
E3	27.0 (3.0)	0.5 (8.6)	F/A + CC (3); F/A + CS (1)
E4	25.7 (3.6)	0.5 (6.3)	F/A + CC (2); F/A + CS (2)
E5	28.1 (2.6)	0.6 (1.9)	F/A + CC (3); F/A +CS (1)
E6	29.4 (4.8)	0.6 (13.4)	F/A+ F/C + CS (3)

Failure modes: F/A = debonding failure at CFRP-Adhesive interface; A/C = debonding failure at adhesive-concrete interface; C = cohesive failure of concrete; A = cohesive failure of adhesive; CC = concrete cracking; CS = concrete splitting; values between brackets are the number of specimens where this failure mode occurred.

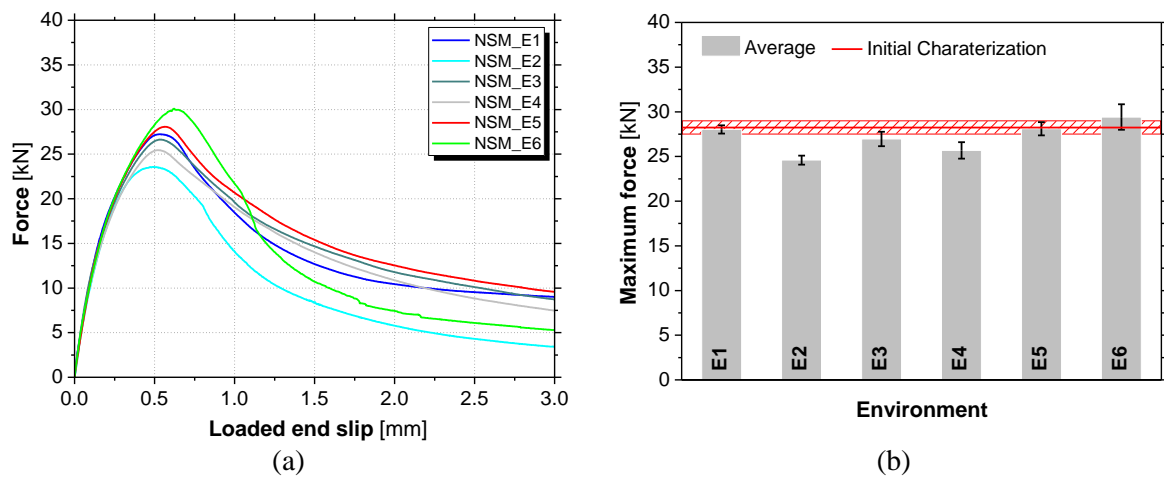


Figure 6. (a) Pull-out force vs. loaded end slip relationships obtained in bond NSM tests in each environment (average of 4 specimens) and (b) maximum pull-out force obtained on bond NSM tests after two years of exposure in each environment, including the initial characterization.

The results of the initial characterization are in agreement with the results obtained in other similar works (Fernandes et al. 2018; Fernandes et al. 2015; Ricardo Cruz et al. 2020). Negligible variations in the values of  $F_{max}$  (-0.7%) were observed when the bond NSM specimens were exposed to E1 environment for two years, indicating a non-reduction of the performance of the adhesive under controlled environment. The two-years immersion in water (E2 environment) led to the greatest reduction in  $F_{max}$  (-12.2% when compared with the reference E1). In addition to the long-term immersion in water, these specimens were tested in a saturated state, which justifies this outcome. As referred



before, the epoxy adhesive absorbs water leading to plasticization and swelling, as mentioned in the literature, e.g. (Cabral-Fonseca et al. 2018; Sousa et al. 2018). A decrease in  $F_{max}$  was also observed in E3 (-3.8%) and E4 (-8.4%). A negligible increase (+0.3%) was observed in E5, while in E6, a higher increase was recorded (+4.9%).

Figure 7 presents the two dominant failure modes observed in bond NSM tests after two years of exposure. These failure modes were classified according where it occurred: (i) concrete – C; (ii) adhesive – A; (iii) interface laminate/adhesive – F/A; or (iv) interface adhesive/concrete – A/C. In some specimens, these failure modes are accompanied by concrete cracking (CC), concrete splitting (CS) or adhesive cracking (AC). Failure mode F/A was observed in all tests, except in the specimens of E2, where a wider range of failure modes were observed (see Table 5). Although the dominant failure mode after the environmental exposure remained the same (F/A), more complex failure modes were observed (combination between F/A and other failure modes).

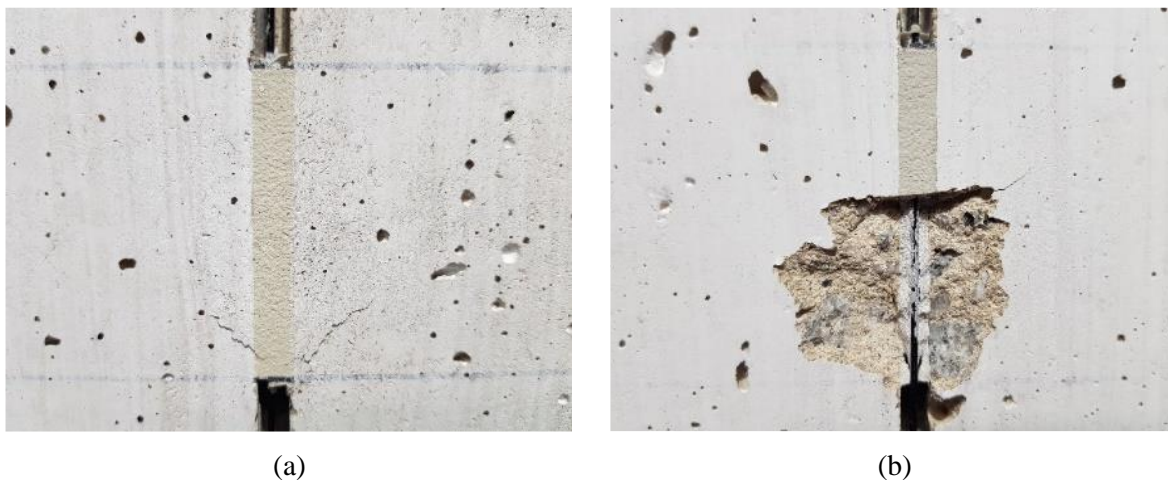


Figure 7. Typical failure modes dominant in bond NSM tests: (a) debonding failure at laminate-adhesive interface with concrete cracking – F/A + CC and (b) debonding failure at laminate-adhesive interface with concrete splitting – L/A + CS.

## 4. Conclusions

This work addressed the durability of bond using two techniques (EBR and NSM) for strengthening of existing reinforced concrete structures under natural ageing. Four outdoor environments to induce ageing, mainly by carbonation (E3), freeze-thaw attack (E4), elevated temperatures (E5), and airborne chlorides from seawater (E6), were considered. A control (reference) environment (E1) and an environment based on the immersion in water under controlled temperature (E2) were also included. The investigation included the assessment of bond between CFRP laminates and concrete at early stage and after two years of exposure. Thus, from the studies carried out, the following main conclusions can be drawn:

- The bond behavior and maximum strength observed on the specimens from the initial characterization were similar to other previous equivalent studies; additionally, the bond strength reached is according to the expected value based on the guidelines;
- After two years of exposure to E1, the EBR bond specimens presented a decrease of -9.5% on the maximum force, whereas in NSM, the variations are negligible;
- After two years of exposure, the maximum force achieved in the specimens of EBR technique of E2-E4 environments increased, between 16.2% and 3.0%, in comparison with the initial characterization; in NSM, there was a decrease in specimens of E2-E5 environments, especially in specimens immersed (-12.8%), while in E6 there was an improvement (+4.3%) of the bond mechanical properties of the specimens;

- The observed failure modes in EBR specimens at the initial characterization and after two years of exposure were similar (cohesive on the concrete); in NSM specimens, the failure modes changed with the exposure.

From these tests, a clear trend has not been obtained, needing more tests with longer periods to better understand the evolution of the long-term variation of bond mechanical properties of the EBR and NSM strengthening techniques under natural ageing.

## Acknowledgements

This work was carried out in scope of the project FRPLongDur POCI-01-0145-FEDER-016900 (FCT PTDC/ECM-EST/1282/2014) funded by national funds through the Foundation for Science and Technology (FCT) and co-financed by the European Fund of the Regional Development (FEDER) through the Operational Program for Competitiveness and Internationalization (POCI) and the Lisbon Regional Operational Program and, partially financed by the project PO-CI-01-0145-FEDER-007633, and partly financed by FCT / MCTES through national funds (PIDDAC) under the R&D Unit Institute for Sustainability and Innovation in Structural Engineering (ISISE), under reference UIDB / 04029/2020. This work is financed by national funds through Foundation for Science and Technology, under grant agreement (SFRH/BD/131259/2017) attributed to the first author. The authors also like to thank all the companies that have been involved supporting and contributing for the development of this study, mainly: S&P Clever Reinforcement Iberia Lda, Portuguese Institute for Sea and Atmosphere, I. P. (IPMA, IP), Hilti Portugal-Produtos e Serviços, Lda., Artecancer – Indústria Criativa, Lda., and Tecnipor - Gomes&Taveira Lda.

## References

- Al-Tamimi Adil, K. *et al.* (2015). Durability of the bond between CFRP plates and concrete exposed to harsh environments. *Journal of Materials in Civil Engineering*, 27: 04014252.
- Bhashya, V. *et al.* (2015). Long term studies on FRP strengthened concrete specimens. *Indian Journal of Engineering and Materials Sciences*, 22, 465-472.
- Cabral-Fonseca, S. *et al.* (2018). Durability of FRP - concrete bonded joints in structural rehabilitation: A review. *International Journal of Adhesion and Adhesives*, 83, 153-167.
- CNR. (2013) CNR-DT 200 R1/2013. Guide for the design and construction of externally bonded FRP systems for strengthening existing structures.
- Fernandes, P. *et al.* (2018). Durability of bond in NSM CFRP-concrete systems under different environmental conditions. *Composites Part B: Engineering*, 138, 19-34.
- Fernandes, PMG., Silva, PM., and Sena-Cruz, J. (2015). Bond and flexural behavior of concrete elements strengthened with NSM CFRP laminate strips under fatigue loading. *Engineering Structures*, 84, 350-361.
- Hassan, SA. *et al.* (2015). Characteristics of concrete/CFRP bonding system under natural tropical climate. *Construction and Building Materials*, 77, 297-306.
- Hsieh, C-T., Lin, Y., and Lin, S-K. (2016). Impact-echo method for the deterioration evaluation of near-surface mounted CFRP strengthening under outdoor exposure conditions. *Materials and Structures*, 50, 72.
- Iovinella, I., Prota, A., and Mazzotti, C. (2013). Influence of surface roughness on the bond of FRP laminates to concrete. *Construction and Building Materials*, 40, 533-542.
- Kabir, MI., Shrestha, R., and Samali, B. (2016). Effects of applied environmental conditions on the pull-out strengths of CFRP-concrete bond. *Construction and Building Materials*, 114, 817-830.
- Mazzotti, C BA. *et al.* Bond between EBR FRP and concrete. In: Pellegrino C, Sena-Cruz J, editors. *RILEM State-of-the-Art Reports*, vol. 19, Dordrecht: Springer Netherlands; 2016, p. 39–96. .
- Mohd Hashim, MH., Mohd Sam, AR., and Hussin, M. (2016). Experimental investigation on the effect of natural tropical weather on interfacial bonding performance of CFRP-concrete bonding system. 11, 584-604.
- Ricardo Cruz, J. *et al.* (2020). Bond behaviour of NSM CFRP laminate strip systems in concrete using stiff and flexible adhesives. *Composite Structures*, 245: 112369.
- Sen, R. (2015). Developments in the durability of FRP-concrete bond. *Construction and Building Materials*, 78, 112-125.
- Soares, S. *et al.* (2019). Influence of surface preparation method on the bond behavior of externally bonded CFRP reinforcements in concrete. *Materials*, 12, 414.
- Sousa, JM., Correia, JR., and Cabral-Fonseca, S. (2018). Durability of an epoxy adhesive used in civil structural applications. *Construction and Building Materials*, 161, 618-633.
- Tatar, J., Hamilton, HR. (2016). Comparison of laboratory and field environmental conditioning on FRP-concrete bond durability. *Construction and Building Materials*, 122, 525-536.